

# Compressibility and Dynamic Properties of Diatomaceous Soils from Mejillones, Chile

Carlos OVALLE<sup>a,1</sup>, Ghio ARENALDI-PERISIC<sup>b</sup> and Antonio BARRIOS<sup>c</sup>

<sup>a</sup>*Research Institute of Mining and Environment (RIME UQAT-Polytechnique),*

*Dep. of Civil, Geological and Mining Eng., Polytechnique Montréal, Canada.*

<sup>b</sup>*Dep. of Structural and Geotechnical Eng., Pontificia Universidad Católica de Chile*

<sup>c</sup>*Petrus Consultores Geotécnicos, Chile*

**Abstract.** This article presents an experimental laboratory study on diatomaceous soil from Mejillones Bay in northern Chile. SEM microscopic observations of the diatom fossils and their mineralogical composition are reported. Despite its low density and high plasticity, the material reaches relatively high yield stress. Over that limit, the soil is highly compressible, presumably due to breakage of the diatom frustules, and presents significant creep strains. Dynamic properties and shear modulus degradation are also reported, where the results of  $G_{max}$  are consistent with values of  $V_s$  measured in-situ.

**Keywords.** Diatomaceous soil, compressibility, creep, microstructure, shear modulus.

## 1. Introduction

The Mejillones Bay, located in the Antofagasta region in northern Chile, has undergone significant industrial and port development over the last 20 years, mainly to provide services to the mining and energy industries. Most of these works are founded on diatomaceous soils, composed by a mixture of sand, fines and fossils of diatoms. This composition gives the soil a singular geotechnical behavior that does not coincide with classical correlations usually applied in geotechnical engineering. In addition, the information reported about the behavior of the undisturbed material is scarce.

Diatoms are single-celled microalgae that constitute one of the most common types of phytoplankton. Its size varies from 10 to 100  $\mu\text{m}$  and has a hard and porous external frustule composed almost entirely by silica [1]. In general, the source of silica comes from volcanic activity, which explains the presence of these soils in sectors adjacent to the Pacific ring of fire; for example Chile, Colombia, Mexico and Japan [1-6]. After its death and organic decomposition, the frustules are deposited at the bottom of the oceans or lakes forming deposits of diatomaceous soils [7]. Due to the internal structure of the fossils, these soils have low dry density, high water content and Atterberg Limits that usually imply a classification of high plasticity silt [1] [8] [9]. However, the soil has high shear strength and relatively high yield stress [2] [3] [6] [8].

---

<sup>1</sup> Corresponding Author: Carlos Ovalle, Dep. of Civil, Geological and Mining Engineering, Polytechnique Montréal, Canada, [carlos.ovalle@polymtl.ca](mailto:carlos.ovalle@polymtl.ca)

This article presents an experimental laboratory study on compressibility and dynamic properties of undisturbed samples of a diatomaceous soil in the Mejillones Bay. The soil microstructure and its mineralogical composition is also reported.

## 2. Geological framework

The site studied corresponds to the peninsula of Mejillones in northern Chile (Figure 1), formed by a morphological relief originated by the accretion of Palaeozoic rocks (570 million of years) to the continent, where the conforming rocks are of the Jurassic (200-145 Ma) and Cretaceous (145-65 Ma), predominantly [11] [12]. Within the main geological units that emerge in this peninsula, the sediments that fill the Mejillones basin correspond to Cenozoic deposits related to Neogene events (25 to 2 Ma), and to recent Quaternary deposits, corresponding to sands, silts, limestones and diatomites, known as formation La Portada [11] [12] [13].

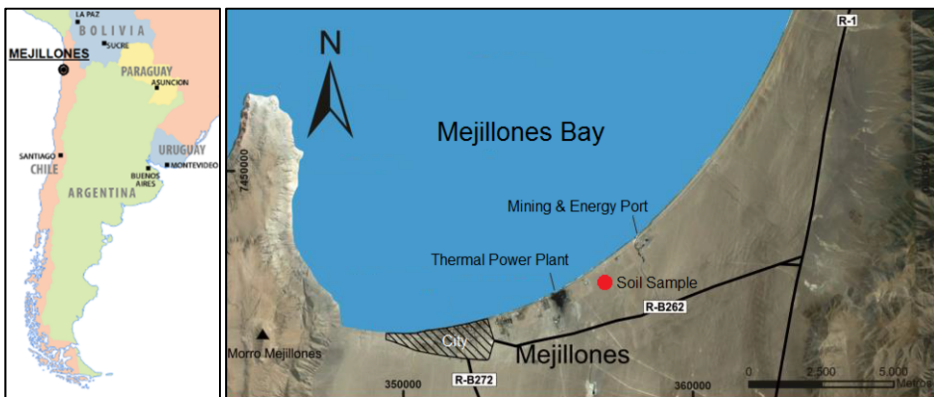
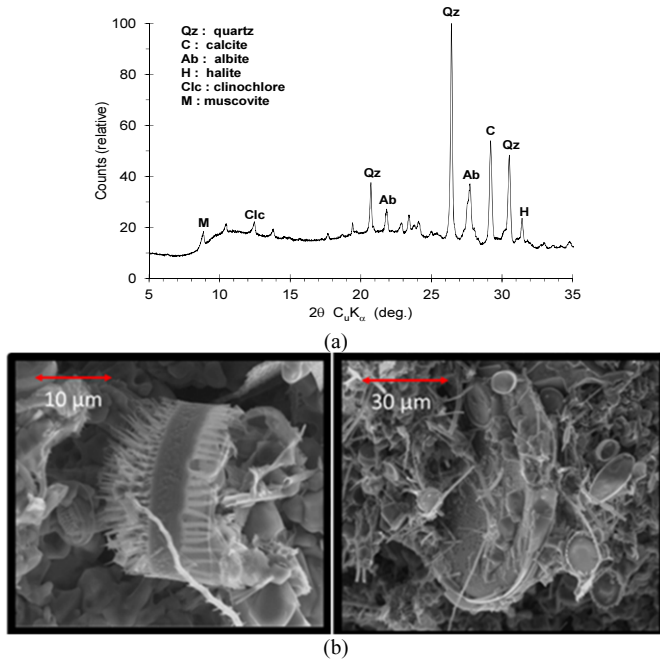


Figure 1. Mejillones Bay (modified from [13]).

Table 1. Geotechnical characterization.

Properties	Results
Liquid limit, $LL$ [%]	82
Plasticity index, $PI$ [%]	38
Classification U.S.C S	MH
Fines content ( $<74 \mu\text{m}$ )	72
Clay content ( $<2 \mu\text{m}$ )	19
Specific Gravity, $G_s$	2.635
Max. Proctor $\gamma_d$ [ $\text{kN}/\text{m}^3$ ]	10.9
Optimum Proctor $w$ [%]	28.5



**Figure 2.** (a) XRD analysis and (b) SEM observations.

### 3. Material

Several undisturbed samples were obtained in the same test pit in the Mejillones Bay (Figure 1), in the form of undisturbed blocks (30 cm cubes) carved at a depth of 3 meters. The material was sealed with plastic film, taken to the laboratory and stored in moist chamber. To characterize the soil, particle size analysis, solid density, Atterberg Limits (wet method), standard Proctor test (wet method), XRD analysis and scanning electron microscope (SEM) observations were performed (Figure 2), with qualitative evaluation of elements by spectroscopy. Geotechnical properties are shown below in Table 1. XRD and SEM confirm that the presence of silica in the form of Quartz is predominant, followed by Calcite and Calcium Albite. The evidence suggest that clay minerals are not a predominant phase in the material.

### 4. Consolidation and creep

A series of oedometrical tests was performed according to ASTM D2435-11 using undisturbed and remolded (moist tamping 3 layers) samples of 50 mm diameter and 16 mm height. Demineralized water flooding saturation was carried out after stabilization of a load of 98 kPa; no swelling or collapse was observed after flooding under constant load. Isotropic consolidation tests were also carried out in saturated samples based on ASTM D4767-04 (drained consolidation at constant back pressure on saturated samples, Skempton  $B > 0.95$ ), using undisturbed cylindrical samples of 50 mm diameter and 100 mm of height.

Table 2 presents, for each sample, the initial dry density  $\gamma_d$ , gravimetric water content  $w$  and the initial void ratio  $e_0$ . Undisturbed samples at natural  $w$ , from 62 to 93%, had  $\gamma_d$  of 6.28 to 7.46 kN/m<sup>3</sup>. Three undisturbed samples were air-dried (in the shade) for 10 days (samples N6, N7 and NI1), reaching  $w$  from 20 to 36% and dry densities from 7.65 to 9.32 kN/m<sup>3</sup>.

Figure 3 shows isotropic and oedometrical compression curves, obtaining an average yield stress of 540 kPa using the Casagrande method ( $\sigma'_v$  is the effective vertical stress for the oedometrical tests and  $p'$  is the effective confinement pressure for isotropic tests). The yield stress value is significantly higher than the overburden pressure (in-situ depth of 3 m), therefore, the apparent overconsolidation of the material should be explained by diagenesis processes [2] [3].

The values of  $C_s$  and  $C_c$  ( $\Delta e / \Delta \log \sigma'$ , recorded at 24 hours under constant load) are presented in Table 2, obtaining an average in undisturbed samples of 0.079 and 0.75, respectively. Based on various empirical results, Terzaghi & Peck [14] proposed the empirical relationship for the compression index  $C_c = 0.009(LL[\%] - 13)$ ; using  $LL = 62\%$  for the material under study is obtained a value of  $C_c = 0.441$ , which is significantly lower compared to what was obtained in this work. Similar conclusions are obtained by using the empirical correlations of Kulhawy & Mayne [15].

The high contrasts between  $C_s$  and  $C_c$  and the high compressibility after yielding would be fundamentally because of the fracture of diatom frustules, generating important irreversible deformations due to the collapse of the soil structure. This is evidenced by several SEM observations of post-test consolidation samples; a couple of examples are shown in Figure 4, where it is clearly observed that the frustules are found massively fractured, similarly with microscopic observations obtained by other authors [2]. Frustules crushing should cause a reorganization of the soil fabric to a denser state under constant stress. Thus, it can be assumed that the mechanical behavior of the diatomaceous soil could be similar to that of granular materials of relatively uniform particle size, in which yielding triggers particle breakage, resulting in large plastic strains [16] [17] [18] [20].

Respectively, Figures 6 and 7 present the evolution of  $C_c$  (at 24 hours) and  $C_\alpha$  (between 1 hour and 24 hours) against each increase of load in undisturbed samples. It is observed that  $C_c$  evolves towards a constant value of 1.0 to 2.0, following a similar trend compared to the carbonated sand (sensitive to the breakage of grains) tested by Mesri & Vardhanabhuti [17]. On the other hand, remolded samples do not have a sudden or abrupt change in compressibility since the previous remolding process could have fractured a significant amount of diatoms, generating a stable internal structure.

**Table 2.** Samples tested.

Sample	Notation	$\gamma_d$ [kN/m <sup>3</sup> ]	$w$ [%]	$e_0$	Yield stress [kPa]	$C_c$ ( <sup>3</sup> )	$C_s$	$C_c/C_s$
Undisturbed, natural water content	N1	7.46	91	2.46	-	-	0.083 <sup>(1)</sup>	-
	N2	7.36	91	2.48	.	-	0.101 <sup>(1)</sup>	-
	N3	6.38	96	3.01	450	1.63	0.104 <sup>(1)</sup>	15.8
	N4	6.18	83	2.44	620	1.77	0.117 <sup>(1)</sup>	15.0
	N5	6.57	93	2.91	450	1.63	0.120 <sup>(2)</sup>	13.6

<sup>1</sup>value obtained in swelling; <sup>2</sup>value obtained in the overconsolidated phase; <sup>3</sup>value obtained in the normally consolidated phase after 24 hours under constant stress.

**Table 2.** (continued) Samples tested.

Sample	Notation	$\gamma_d$ [kN/m <sup>3</sup> ]	$w$ [%]	$e_0$	Yield stress [kPa]	$C_c$ ( <sup>1</sup> )	$C_s$	$C_c/C_s$
Undisturbed, natural water content	N1	7.46	91	2.46	-	-	0.083 <sup>(1)</sup>	-
	N2	7.36	91	2.48	.	-	0.101 <sup>(1)</sup>	-
	N3	6.38	96	3.01	450	1.63	0.104 <sup>(1)</sup>	15.8
	N4	6.18	83	2.44	620	1.77	0.117 <sup>(1)</sup>	15.0
	N5	6.57	93	2.91	450	1.63	0.120 <sup>(2)</sup>	13.6
Undisturbed, shadow-dried during 10 days	N6	7.65	20	2.37	350	0.98	0.092 <sup>(1)</sup>	10.7
	N7	8.53	22	2.00	400	1.10	0.032 <sup>(1)</sup>	34.0
	NI1	9.32	36	1.75	700	1.27	0.039 <sup>(2)</sup>	32.5
Undisturbed, natural water content	NI2	8.24	63	2.12	700	1.28	0.035 <sup>(2)</sup>	37.1
	NI3	6.28	62	3.05	650	2.04	0.07 <sup>(2)</sup>	26.8
Remolded	R1	10.59	35	1.41	-	-	-	-
	R2	7.65	43	2.34	-	-	-	-
	R3	6.28	43	3.07	-	-	-	-

<sup>1</sup>value obtained in swelling; <sup>2</sup>value obtained in the overconsolidated phase; <sup>3</sup>value obtained in the normally consolidated phase after 24 hours under constant stress.

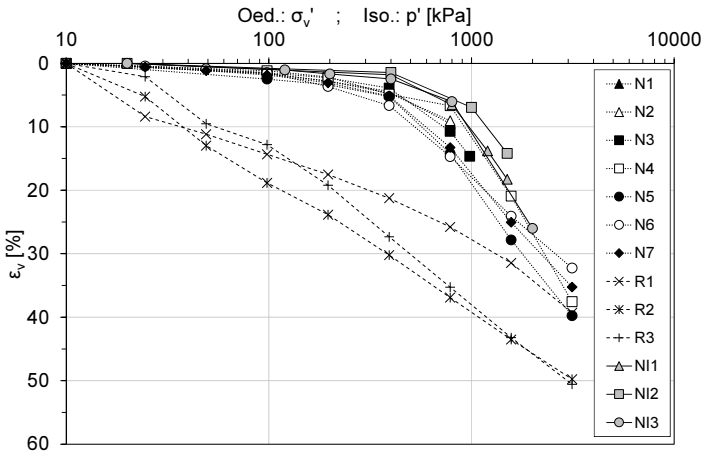


**Figure 3.** Oedometrical and isotropic consolidation curves.

**5. Secondary consolidation**

In order to estimate the end of primary consolidation, excess pore pressure ( $\Delta u$ ) was monitored during isotropic consolidation tests, dissipating by 95% in approximately 60 minutes (after an effective confinement increase from 1000 to 1500 kPa). Similar results were obtained in other isotropic tests, so it is reasonable to assume that secondary consolidation begins after 1 hour under constant stress.

Figure 5 shows the increase of deformation by creep with respect to the 24-hour compression curve at different consolidation times (5 to 50 days), where it is observed

that the deformation rate increases significantly after yielding, reaching even volumetric differences of 3% between 1 and 50 days at constant stress.

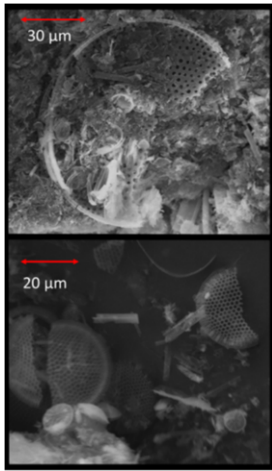


Figure 4. Fractured frustules found in post-testing consolidation samples.

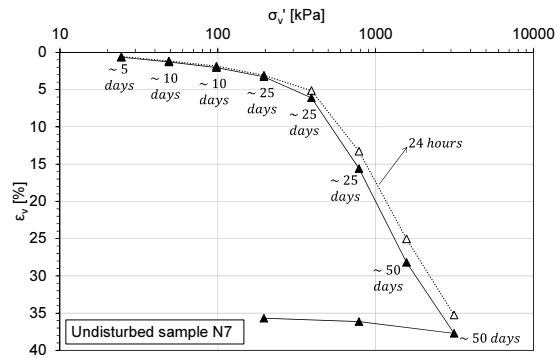


Figure 5. Consolidation after 24 hours and 5 to 50 days (sample N7).

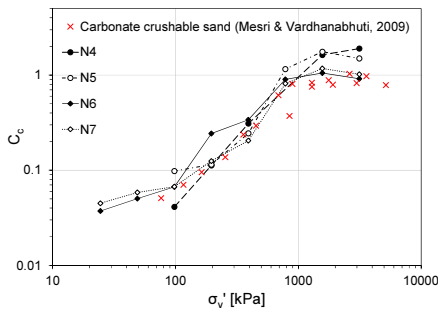


Figure 6. Evolution of  $C_c$ .

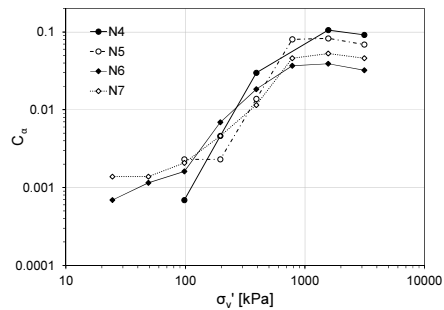


Figure 7. Evolution of  $C_\alpha$ .

## 6. Shear modulus degradation

A series of resonant column (RC), cyclic torsion (CT) and cyclic triaxial (CycTx) tests were performed on undisturbed 50 mm and 100 mm high samples at confinements of 100, 200, 400, 600 and 650 kPa, ensuring saturation at  $B > 95\%$ . The shear modulus ( $G$ ) degradation and damping ( $D$ ) curves are presented in Figure 8. Significant degradation of  $G$  is observed from a shear deformation of  $\gamma=0.01\%$ , whereas in classical literature curves for fine soils [21] and sands [22] this trend typically starts at 0.001%. On the other hand, at  $\gamma$  higher than 0.3% the diatomaceous soil resembles the degradation curves of fine plastic soils ( $PI = 15$  to 30). The material degradation is not affected by effective confinement, which is similar to classical results in fine plastic soils [23].

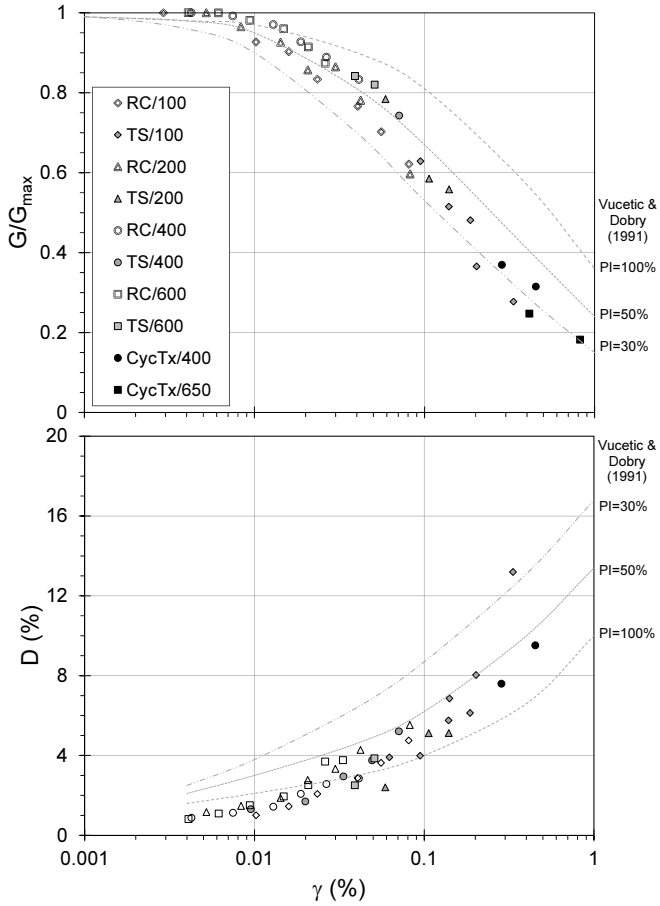


Figure 8. (a) Shear modulus degradation and (b) damping curves (Legend: Test/Confining pressure in kPa).

As shown in Figure 9, the values of  $G_{max}$  obtained in this study are in the same range as the results reported by [12] using in-situ geophysical methods.

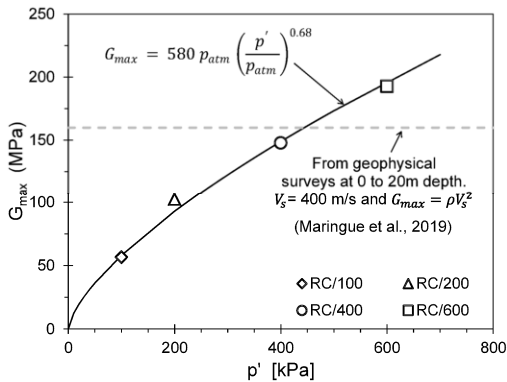


Figure 9.  $G_{max}$  against effective mean pressure  $p'$  (Legend: Test/Confining pressure in kPa).

## 7. Conclusions

SEM microscopic observations show that the diatomaceous soil of Mejillones contains a large quantity of fossilized diatomaceous frustules, with a highly rough surface, various shapes and siliceous material. These particles would be responsible for the high porosity and water content of the soil in its natural condition. Due to the unique properties given by diatom frustules, the classical empirical correlations in the literature for fine soils do not coincide with the behavior of the diatomaceous soils.

From oedometrical and isotropic compression tests, an average  $C_c$  compressibility index of 1.17 and an average yield stress of 540 kPa were obtained. The overconsolidation would be associated to diagenesis processes since the studied material was extracted from 3 m depth test pits. Microscopic observations on tested samples suggest that high compressibility is partially explained due to massive frustules breakage. In addition, for stress higher than the yield stress, creep strains are significant, with volumetric strain of up to 3% at constant stress between 1 and 50 days.

The shear modulus degradation is virtually not affected by effective confinement and it is significantly stiff ( $0.98 G_{max}$ ) up to shear strains of around 0.01%, and does not match empirical correlations for fine soils. After this value, the material is degraded reaching proper values of fine soils. The values of  $G_{max}$  are consistent with results of  $V_s$  obtained in-situ by geophysical methods.

## Acknowledgements

This study is part of the FONDECYT 11150084 project, financed by CONICYT.

## References

- [1] Díaz-Rodríguez, J. A., & González-Rodríguez, R. (2013). *Influence of diatom microfossils on soil compressibility*. In Proceedings of the 18th International Conference on Soil Mechanics and Geotechnical Engineering, Paris.
- [2] Hong, Z., Tateishi, Y., & Han, J. (2006). *Experimental study of macro-and microbehavior of natural diatomite*. Journal of Geotechnical and Geoenvironmental Engineering, 132(5), 603-610.
- [3] Sánchez, M. A. (2002). *Caracterización geomecánica de diatomeas*. Tesis para optar al título de Ingeniero Civil. Departamento de Ingeniería Civil de la Universidad de Chile, Santiago, Chile.
- [4] Verdugo, R. (2008). Singularities of geotechnical properties of complex soils in seismic regions. Journal of geotechnical and geoenvironmental engineering, 134(7), 982-991.
- [5] Wesley, L. D. (2010). Discussion of "Singularities of Geotechnical Properties of Complex Soils in Seismic Regions" by Ramon Verdugo. Journal of geotechnical and geoenvironmental engineering, 136(1), 277-279.
- [6] Arenaldi-Perisic, G., Ovalle, C., Barrios, A. (2019): Compressibility and creep of a diatomaceous soil. Engineering Geology 258(105145) (DOI: 10.1016/j.enggeo.2019.105145).
- [7] Treguer, P., Nelson, D. M., Van Bennekom, A. J., DeMaster, D. J., Leynaert, A., & Quéguiner, B. (1995). *The silica balance in the world ocean: a reestimate*. Science, 268(5209), 375-379.
- [8] Nazar, R., Ovalle, C., Barrios, A., & Arenaldi, G. (2016). Caracterización geotécnica y resistencia al corte de suelos diatomáceos y de la interfaz suelo-acero. En IX Congreso Chileno de Ingeniería Geotécnica, Valdivia, 5-7 de Diciembre de 2016.
- [9] Shiwakoti, D. R., Tanaka, H., Tanaka, M., & Locat, J. (2002). Influences of diatom microfossils on engineering properties of soils. Soils and Foundations, 42(3), 1-17.
- [10] Nava, T. (2007). Influencia de las diatomeas en la resistencia al corte del caolín. Tesis de Maestría. Facultad de ingeniería, Universidad Nacional Autónoma de México, México.

- [11] Muñoz, E., & Rivas, M. (2012). *Modificación plan regulador comunal de Mejillones, zona urbana consolidada y portuaria Mejillones*. Gobierno de Chile.
- [12] Maringue, J., Yañez, G., Sáez, E., Podestá, L., Figueroa, R., Estay, N., Lira, E. (2018). Dynamic characterization of the Mejillones Basin in northern Chile, using combined geophysical field measurements. *Engineering Geology* 233 (2018) 238–254.
- [13] González, J. (2013). *Geología y estructura submarina de la Bahía de Mejillones: su vinculación con la deformación activa en la plataforma emergida a los 23°S*. Memoria para optar al título de Geólogo. Facultad de Ingeniería y Ciencias Geológicas. Universidad Católica del Norte, Antofagasta, Chile.
- [14] Terzaghi, K., & Peck, R.B. (1967). *Soil Mechanics in Engineering Practice*. John Wiley & Sons, New York.
- [15] Kulhawy, F. H., & Mayne, P. W. (1990). *Manual on estimating soil properties for foundation design*. Geotechnical Engineering Group.
- [16] Biarez, J., & Hicher, P. Y. (1994). Elementary mechanics of soil behaviour: saturated remoulded soils. A.A. Balkema.
- [17] Mesri, G., & Vardhanabhuti, B. (2009). Compression of granular materials. *Canadian Geotechnical Journal*, 46(4), 369-392.
- [18] Ovalle, C (2013): Contribution à l'étude de la rupture des grains dans les matériaux granulaires. Ph.D. Thesis, École Centrale de Nantes, France (in french, pdf available on-line: <https://tel.archives-ouvertes.fr/tel-00979827/document>).
- [19] Mesri, G., & Castro, A. (1987).  $C\alpha/Cc$  concept and  $K_0$  during secondary compression. *Journal of Geotechnical Engineering*, 113(3), 230-247.
- [20] Ovalle, C. (2018). Role of particle breakage in primary and secondary compression of wet and dry sand. *Géotechnique Letters*, 8(2), 161-164.
- [21] Vucetic, M., & Dobry, R. (1991). Effect of soil plasticity on cyclic response. *Journal of geotechnical engineering*, 117(1), 89-107.
- [22] Seed, H. B., & Idriss, I. M. (1970). Soil moduli and damping factors for dynamic response analysis. Earthquake Engineering Research Center. University of California, Berkeley, California.
- [23] Ishibashi, I., & Zhang, X. (1993). Unified dynamic shear moduli and damping ratios of sand and clay. *Soils and Foundations*, 33(1), 182-191.